HTML ABSTRACT + LINKS

Epitaxial growth and surface modeling of ZnO on *c*-plane Al_2O_3

T. E. Murphy, S. Walavalkar, and J. D. Phillips
Department of Electrical Engineering and Computer Science, University of Michigan, Ann Arbor, Michigan 48109-2122

(Received 23 June 2004; accepted 10 November 2004)

The growth of ZnO on *c*-plane sapphire by molecular beam epitaxy is presented for varying ratios of zinc and oxygen flux. Reflection high energy electron diffraction patterns during epitaxial growth suggest clear differences in the evolution of surface morphology for differing Zn flux. Atomic force microscope images indicate sizable hexagonal features in the surface morphology for Zn-rich material. A stochastic growth model is presented to represent the experimental ZnO surface, where differences in adatom lateral diffusion length are suspected to be the cause of the differing surface morphology. © *2004 American Institute of Physics*. [DOI: 10.1063/1.1842357]

ZnO has recently received much attention as a wide band-gap direct semiconductor due to its potential as an active material for ultraviolet (UV) optoelectronic devices and electronic device applications requiring high breakdown strength, high temperature operation, or transparency in the visible region. Several techniques of achieving high-quality ZnO thin films have been reported, including molecular beam epitaxy (MBE),[1] metalorganic chemical vapor deposition (MOCVD),[2] and pulsed-laser deposition (PLD).[3] Advanced epitaxial growth techniques such as MBE and MOCVD are needed to achieve ZnO material with controlled thickness and doping profiles for optoelectronic device structures. These techniques also provide precise control of the II/IV ratio which has been shown to be a critical factor in the crystallographic, optical, and electrical properties of the grown films, often demonstrating a clear correlation with surface morphology.[4–6] In these previous studies, O-rich growth has been shown to result in large hexagonal structures, with Zn-rich growth resulting in smaller hexagonal structures, and stoichiometric growth resulting in smooth surfaces with finite roughness. In this work, a more detailed examination of surface morphology is presented for Zn rich and stoichiometric growth conditions. The surface morphologies for the two cases are compared, and a model for diffusion limited epitaxial growth is presented to explain the observed behavior.

The layers studied in this work were grown on *c*-plane sapphire substrates using plasma-assisted molecular beam epitaxy (MBE). The material was grown in a Riber 32P MBE system using atomic oxygen provided by an Oxford Scientific electron cyclotron resonance source, and elemental Zn provided by a standard effusion cell. For this experiment, the O_2 flow rate was maintained at a constant 4 sccm, while the Zn flux was varied by adjusting the temperature of the effusion cell. The ECR power was maintained at 270 W. During growth, the film quality was monitored by reflection high-energy electron diffraction (RHEED). The low temperature buffer process proposed by Tampo *et al.*[7] was used to facilitate high-quality crystalline growth. Following the anneal step, all films showed streaky ZnO RHEED patterns characteristic of a smooth growth surface. Growth was then initiated with the appropriate Zn/O ratio for the experiment. The Zn-rich growth condition, corresponding to a beam equivalent pressure (BEP) of 2.2×10^{-6} Torr, resulted in the observed RHEED pattern rapidly changing from the streaky pattern of the buffer layer to a spotty pattern characteristic of three-dimensional growth and a rough surface. The stoichiometric growth condition, corresponding to a BEP of 5.5×10^{-7} Torr, resulted in the retention of the streaky pattern throughout growth. Figure 1 shows the RHEED patterns observed with both Zn rich and stoichiometric growth conditions for the ZnO $[11\bar{2}0]$ reflection.

Following growth, the structural and electronic properties of the layers were determined by x-ray diffraction, Hall effect measurements, reflectance spectrometry, and wet chemical etching. The thickness of the layers was determined using reflectance spectrometry to be ~380 and 800 nm for the stoichiometric and Zn-rich samples, respectively, corresponding to a growth rate of ~0.10 and 0.18 μm/h. X-ray diffraction rocking curves of the (0002) ZnO peak showed full width at half maximum values of ~800 arcsec. Hall effect measurements indicated *n*-type material with carrier concentration of $\sim7\times10^{17}$ cm^{-3} and electron mobility of 50 cm^2/Vs for the stoichiometric sample while the Zn-rich sample had carrier concentration of 3×10^{18} cm^{-3} and electron mobility of 38 cm^2/Vs. The polarity of the layers was determined to be O face by 1% nitric acid etching.[8] These

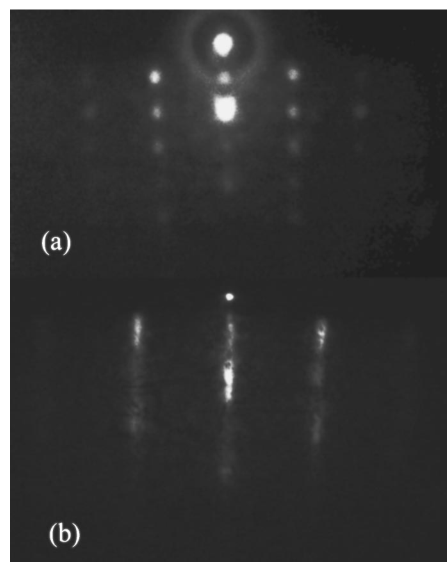

FIG. 1. RHEED patterns from $[11\bar{2}0]$ ZnO during MBE growth under (a) Zn-rich and (b) near-stoichiometric conditions.

 © 2004 American Institute of Physics

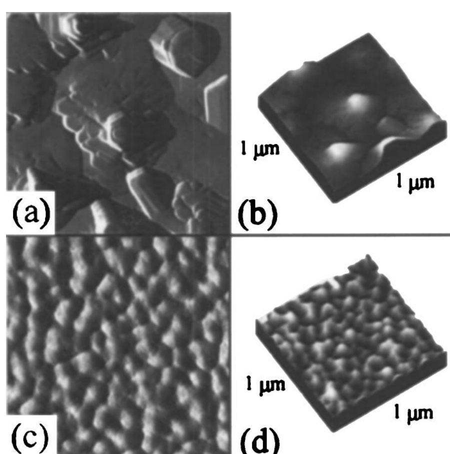

FIG. 2. AFM images of a 1 μm×1 μm area of a ZnO surface grown under (a) and (b) Zn-rich conditions and (c) and (d) stoichiometric conditions.

structural and electronic characteristics are similar to previous reports of ZnO growth on sapphire by molecular beam epitaxy.[4–6]

The surface morphology of the ZnO layers was investigated by atomic force microscopy (AFM), as shown in the 1 μm×1 μm scans in Fig. 2. The root mean square (rms) roughness of the Zn-rich layer was determined to be ~83 nm, while the roughness of the stoichiometric layer was determined to be only about 4 nm, more than an order of magnitude difference. The Zn-rich surface is dominated by large triangular or hexagonal features of height >50 nm and diameter >100 nm with smooth regions in between, resulting in a dull surface as observed by the naked eye. This seems to indicate selective three-dimensional growth along the *c*-axis. The layer grown near stoichiometric conditions has very small features indicative of two-dimensional growth, with a shiny surface observed by the naked eye. The observed surface morphology is consistent with the spotty and streaky RHEED patterns observed for the Zn-rich and stoichiometric samples, respectively.

The formation of clusters or mounds altering the surface morphology during epitaxial growth may be due to instabilities driven by strain, crystallographic orientation, or other mechanisms. The evolution of surface morphology during MBE growth may be effectively modeled using stochastic simulations, where good agreement has been observed with experiment.[9,10] These stochastic models begin with a set of "rules" governing growth, where proper modeling of the growth mechanism of interest provides a means of predicting trends caused by physical growth parameters. In this work, a stochastic growth model is used to examine the effect of varying lateral adatom diffusion length on surface morphology to model the observed ZnO surfaces under varying Zn/O flux ratio. The Das Sarma–Tamborenea (DT) model is used to represent a simplistic limited mobility nonequilibrium model for MBE growth.[9,10] In this model, an adatom is randomly dropped on a surface. If this adatom has at least one nearest neighbor (coordination number of 2 or more), it is incorporated into that site. If the adatom does not have a lateral nearest neighbor at the deposition site, it is allowed to search within a finite diffusion length to a final site with a higher coordination number. If a higher coordination number is not found within this lateral diffusion length, the adatom is incorporated into the crystal at the original deposition site. This model is similar to the prediction for ZnO growth along the *c*-axis under O-rich (small diffusion length) or Zn-rich (large diffusion length) conditions. A Zn atom on the O face of the growing crystal will have a single bond to an oxygen atom beneath it. The Zn atom will be stabilized when there is a neighboring Zn atom and both atoms bond to an oxygen atom from the next higher monolayer. Stable and unstable configurations are shown schematically in the two-dimensional representation in Fig. 3.

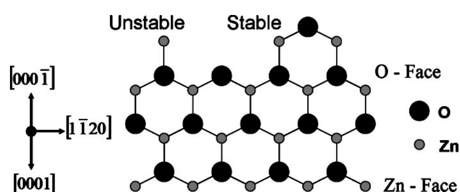

FIG. 3. Two-dimensional illustration of the ZnO crystal structure and stable and unstable configurations for Zn adatom positions.

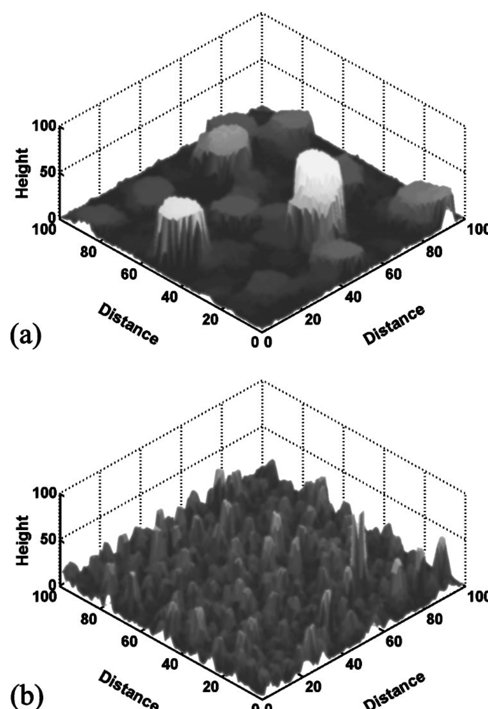

FIG. 4. Simulation of the growth of 10 monolayers (ML) on a 100×100 lattice using the DT model with (a) large and (b) small lateral diffusion length.

The DT stochastic growth model was used on a 100 ×100 square grid to compare surface morphology for varying adatom diffusion lengths. This approach will enable the comparison of trends with diffusion length, and should not be used for quantitative comparisons due to at least two important inaccuracies. The first is that a square grid is used for simplicity, where a hexagonal grid would be needed to truly represent surface morphology. The second is that the grid represents a more macroscopic scale than the true scale of crystal growth. The 100×100 grid will be used to represent a 1 μm square region of growth, where an ~3000×3000 grid would be needed to represent adatoms at the true atomic spacing. The reduction in grid size is used to make the calculations tractable. Simulations were performed for varying lateral diffusion lengths for 10^5 adatoms, corresponding to 10 monolayers (ML) of growth. The resulting surface profiles for lateral diffusion length of 2 and 80, in arbitrary

units, are shown in Fig. 4. The resulting surface morphologies show remarkable resemblance to the observed AFM images in Fig. 2. The AFM image for the near stoichiometric growth [Figs. 2(c) and 2(d)] shows good agreement with the DT model with small diffusion length [Fig. 4(b)], where a relatively smooth surface morphology with regular surface undulations is observed. The AFM image for Zn-rich growth [Figs. 2(a) and 2(b)] shows good agreement with the DT model with large diffusion length [Fig. 4(a)]. One interpretation for a potential increase in lateral adatom diffusion length for Zn-rich growth is that there is relative deficiency of reactive oxygen present to bond with two adjacent Zn atoms. In this situation, there is not a stable crystalline configuration, allowing Zn adatoms to continue to migrate. One distinct difference between the DT model and the observed experimental surface for this condition is the triangular or hexagonal structure observed by AFM. The shape of the experimental features may be more accurately modeled in the simulation through the incorporation of a hexagonal lattice and/or incorporating new rules in the stochastic model to account for lateral growth rate differences along defined crystalline directions corresponding to bond angles (i.e., faceted growth). The observation of the large features for larger lateral diffusion length suggests that the achievement of a smooth surface morphology for ZnO growth requires near stoichiometric flux conditions along the c-axis or growth on alternative crystalline orientations that are nonpolar.

In conclusion, RHEED patterns developing during the MBE growth of ZnO show clear differences between growth under Zn rich and stoichiometric flux conditions. These differences are shown to correspond to the nanoscale surface morphology of the grown layers observed by AFM. Using a stochastic growth model, the surface morphology resulting from changes in Zn/O ratio can be predicted based on differences in lateral adatom diffusion length. The predictions of the model show good agreement with experimental AFM measurements.

This project was supported by the Center for Optoelectronic Nanostructured Semiconductor Technologies, a DARPA UPR award HR0011-04-1-0040, and the Rackham Graduate School at The University of Michigan.

[1] Y. F. Chen, D. M. Bagnall, H. J. Ko, K. T. Park, K. Hiraga, Z. Zhu, and T. Yao, J. Appl. Phys. **84**, 3912 (1998).
[2] T. Shiosaki, T. Yamamoto, M. Yagi, and A. Kawabata, Appl. Phys. Lett. **39**, 399 (1981).
[3] R. D. Vispute, V. Talyansky, Z. Trajanovic, S. Choopun, M. Downes, R. P. Sharma, M. C. Woods, R. T. Lareau, K. A. Jones, and A. A. Iliadis, Appl. Phys. Lett. **70**, 2735 (1997).
[4] K. Sakurai, M. Kanehiro, K. Nakahara, T. Tanabe, S. Fujita, and S. Fujita, J. Cryst. Growth **209**, 522 (2000).
[5] Y. Chen, H. Ko, S. Hong, T. Yao, and Y. Segawa, Appl. Phys. Lett. **80**, 1358 (2002).
[6] H. Kato, M. Sano, K. Miyamoto, and T. Yao, Jpn. J. Appl. Phys., Part 1 **42**, 2241 (2003).
[7] H. Tampo, A. Yamada, P. Fons, H. Shibata, K. Matsubara, K. Iwata, K. Nakahara, and S. Niki, Phys. Status Solidi C **1**, 888 (2004).
[8] A. Mariano and R. Hanneman, J. Appl. Phys. **34**, 384 (1963).
[9] S. Das Sarma and P. Tamborenea, Phys. Rev. Lett. **66**, 325 (1991); P. Tamborenea and S. Das Sarma, Phys. Rev. E **48**, 2575 (1993).
[10] P. Chatraphorn, Z. Toroczkai, and S. Das Sarma, Phys. Rev. B **64**, 205407 (2001).